Journal of Nuclear Materials 408 (2011) 73–89

Contents lists available at ScienceDirect

Journal of Nuclear Materials

journal homepage: www.elsevier.com/locate/jnucmat

A 25-year laboratory experiment on French SON68 nuclear glass leached in a granitic environment – First investigations

C. Guittonneau [a], S. Gin [a,*], N. Godon [a], J.P. Mestre [a], O. Dugne [b], P. Allegri [b]

[a] CEA Marcoule DTCD/SECM/LCLT, BP 17171, 30207 Bagnols-sur-Cèze Cedex, France
[b] CEA Marcoule DTEC/SGCS/LMAC, BP 17171, 30207 Bagnols-sur-Cèze Cedex, France

ARTICLE INFO

Article history:
Received 22 July 2010
Accepted 31 October 2010

ABSTRACT

We have investigated a 25.75-year old leaching experiment to improve our understanding of the mechanisms controlling glass dissolution in geological disposal conditions. A SON68 glass block was leached in slowly renewed synthetic groundwater (at 90 °C, 100 bar) in contact with some pieces of granite and Ni–Cr–Mo alloy as environmental storage materials. One hundred and sixty-three samplings were carried out over the entire duration of the experiment and were used to calculate the mean thickness of the altered glass (28 (±9) μm) and the glass dissolution rate. After few months, the rate remained very constant at 6×10^{-3} g m^{-2} d^{-1} which is about 20 times higher than the residual rate measured in a batch reactor at the same temperature.

At the end of the experiment, mainly SEM analyses were performed on the entire glass block. Surprisingly, the glass alteration layer has neither a homogeneous thickness, nor a homogeneous morphology. The location of the sampling valve (at half height of the glass block) seems to divide the glass block into two parts. In the upper half (above the sampling valve), the general morphology of the alteration layer consists in a relatively simple and uniform gel and some secondary phases which are rare-earth phosphates. The mean measured thickness of this alteration layer is 6.7 (±0.3) μm. However, in the lower half of the glass block, the gel is globally larger and frequently contains rounded shapes which are rare-earth phosphates. This section is edged by secondary phases bearing Mg, Na, Zn and Ni. The mean measured thickness is 81.3 (±1.1) μm in the lower half. In this experiment, the flow rate which leads to the hydrodynamic transport of the soluble species must be a key factor for the local glass alteration process. We have also shown that this unexpected behavior is likely due to heterogeneities of the chemistry of the solution. This conclusion is supported by the behavior of Mg. This element, supplied by the inlet solution, precipitates with Si and forms clay minerals and therefore weakens the passivating properties of the gel. Mg-rich clay minerals are only observed in the lower half of the glass block. Further investigations are necessary to better understand the coupling between the hydrodynamics and chemistry in this experiment. However, based on this study, we can conclude that glass in disposal should be very sensitive to the water renewal near the glass surface.

1. Introduction

Over decades, borosilicate glass has been produced in order to confine high-level radioactive waste from spent nuclear fuel reprocessing. Considering the time required to achieve a low residual radioactivity, typically dozens of thousands of years, providing a final geological disposal site in a deep and stable rock seems to be the best option to guaranty safety over such a long period of time. Based on safety criteria, the most important phenomena that must be thoroughly investigated are the release of radionuclides from the glass matrix due to alteration by groundwater and their migration through the host rock. In a normal or accidental scenario, such phenomena will occur in a "geological-type time frame" before the radionuclides reach the near-surface aquifers. For this reason, a complete methodology is required in such cases, including a laboratory experiment to investigate chemical processes at different scales, a mechanistic model to predict the source term of the radionuclides and a model validation by natural or archaeological analogs, integrated mockups or in situ tests. The present study focuses on a very long laboratory-integrated test devoted to the validation of mechanistic models used to predict glass dissolution rates in a geological repository.

France, like other countries, intends to store high-level and intermediate-level waste in a clay formation. This option has been decided recently (Act dated the 28th of June 2006). The current

* Corresponding author.
E-mail address: stephane.gin@cea.fr (S. Gin).

0022-3115/$ - see front matter © 2010 Elsevier B.V. All rights reserved.
doi:10.1016/j.jnucmat.2010.10.075

disposal concept studied by ANDRA is based on three containment barriers including a glass package (within its primary canister, a stainless steel container), a 55-mm thick carbon steel overpack and, finally, a host rock, which would be a 130-m thick argillite layer dated from the Callovo-Oxfordian period [1] located at 450 m below the surface. In the past, other kinds of host rocks have been investigated such as granite or salt [2–5].

Leaching of silicate and borosilicate glass has been extensively studied. In addition to the simple dissolution process or leaching complex, coupled phenomena occur [6] such as hydration due to water diffusion through the glass structure [7], ion exchange, also called interdiffusion, corresponding to a preferential exchange between alkali from the glass and hydrogen species from the solution [8–10], and hydrolysis of the ionocovalent bonds in the silicate network [11,12]. At a high reaction progress, parts of the hydrolyzed species recondense to form a low-porosity, amorphous and hydrated material, called a gel that progressively restricts water accessibility to the pristine glass [13–16]. According to experimental conditions, the gel is more or less protective [17,18]. One key point is that the main elements of the gel (Si, Al, ...) can be consumed by the precipitation of secondary crystalline phases [16,19]. These secondary phases are mainly phyllosilicates or calcium and rare-earth phosphates [6,20–23] for a temperature below 150 °C.

Like the modifier cations of the glass network, boron is released from the glass and not retained in the alteration products (gel and crystalline phases). Therefore, boron is considered as a good glass dissolution tracer [24].

In most of nuclear glass leaching experiments, glass transforms into a gel which takes up almost the entire volume of the altered glass [21]. This type of glass dissolution is referred to as isovolumetric. However in some specific cases, the gel dissolves rapidly or does not form. This can be the case when glass is altered in direct contact with fresh clay rich in organic matter (Boom clay or FoCa7) [25].

The water chemistry [13,26,27], glass composition [28–32] and physico-chemical conditions (pH [33,34], temperature [35], S/V ratio [36,37], flow rate [38] are key factors for glass leaching, in particular regarding the nature, morphology, and protective effect of the gel layer [18] and the nature of the secondary phases. For example, the presence of HPO_4^{2-} ions in the leachant causes the precipitation of a certain amount of Ca phosphates and rare-earth phosphates. As a result, a higher dissolution rate is maintained compared to the rate achieved without these ions [39]. This is probably due to the loss of Ca from the gel [40]. Furthermore, the presence of Si in the leachant enhances the passivating effect of the gel, as silicon is the main gel former [18].

Moreover, the nature of the environmental materials is also very important, as they can be the site of adsorption/desorption-type or dissolution/precipitation-type phenomena, which modify the composition of the solution. In presence of clay as a host rock in a deep geological storage, the dissolution rate of the glass is increased since clay adsorbs forming elements of the gel layer (Si, Al, Ca) [41,42]. Furthermore, Si from the glass can slowly precipitate on the Boom clay [24].

Some studies concern a granitic environment. From a general point of view, it is believed that granite limits glass dissolution [4,43–45]. Hermansson et al. explain that the influence of granite on the glass leaching rate is mainly due to affinity effects. In a granitic medium, groundwater supplies dissolved silica which, as explained above, contributes to decreasing the glass dissolution rate due to its condensation into a gel.

Only very few long-term experiments have already been published. One of these experiments has been carried out with a high-level waste (HLW) glass which was buried during 24 years in a lysimeter in aim of studying the radioactive distribution of alpha and beta emitters, and ^{137}Cs [46]. The studied glass contained less B_2O_3 and more Al_2O_3, Fe_2O_3 and Na_2O than the SON68 glass, and the burial soil was a Fe_2O_3 rich clay providing oxidizing conditions. The glass characterization evidenced an alteration layer depleted in Na, Ca and Mn and relatively enriched in Si, Al and Fe. The minor secondary phases were gibbsite and/or boehmite. The thickness of this layer was around 8 μm, with a maximal value of 32 μm in some regions. The mean value of the glass alteration thickness leads to a mean alteration rate of about 2.5×10^{-3} g m^{-2} d^{-1}. Assuming a mean temperature around 15 °C, one may conclude that the glass has been dissolved near its maximum dissolution rate during such a long period of time. It should be interesting to confirm this result and try to understand the reasons of such a behavior.

The present study concerns a long-term laboratory experiment devoted to validating our understanding of the phenomenology in a realistic environment. The experiment has been carried out over a period of 25.75 years in a granitic environment where glass alteration in synthetic groundwater and water renewal phenomena occur at quite a high temperature (90 °C). Environmental materials such as sand, corrosion products and granite coupons are also present near the glass block. This study concerns a geological repository after rapid corrosion and the mechanical failure of a steel canister. Even if a granitic environment is not yet considered as the reference host rock in France, this unique long-term experiment is a good solution for validating mechanistic models such as GM2001 [47] or GRAAL [6,16,48], and will contribute to improving our understanding of the overall glass leaching mechanism in deep geological storage conditions.

This study includes a multiscale characterization of the altered glass in order to address several questions. Considering the geometry of the experiment, is the glass alteration homogeneous or not? What is the fate of the protective gel which has formed once the solution near the glass is saturated with respect to silica? What is the main driving force controlling the long-term glass dissolution rate? Flow rate, synthetic groundwater composition, chemical interactions between glass and sand, granite or corrosion products, or other forces? Does this long time frame modify our current understanding of the glass dissolution phenomenon? In this study, we performed an in-depth characterization of the altered glass block based on the gel thickness and composition and according to its location in the block, to the nature of the secondary crystalline phases, and also to the alteration of materials surrounding the glass. Data obtained at a microscopic level were then pooled to be compared with the average behavior determined from the leaching data. We specifically focused on the behavior of magnesium, considering that the glass is Mg free, that Mg is supplied by the leachant solution, and that Mg is known to enhance the glass dissolution process resulting from secondary clay mineral precipitation [29,49,50].

2. Materials and methods

2.1. Experimental setup

The experiment consists in the alteration of SON68 glass at 90 °C and under a hydrostatic pressure of 100 bar, when in contact with environmental materials (sand and pieces of granite and Ni–Cr–Mo alloy) and water which has been initially equilibrated with the environmental materials. This experiment was performed with two cells mounted in series (see Fig. 1). The preconditioning vessel contained the environmental materials (granite and sand). The upper cell was the leaching vessel. The glass block was placed in this cell and surrounded with the environmental materials, particularly with sand and with some pieces of granite and Ni–Cr–Mo alloy. The granite coupons simulated the host rock of the geological

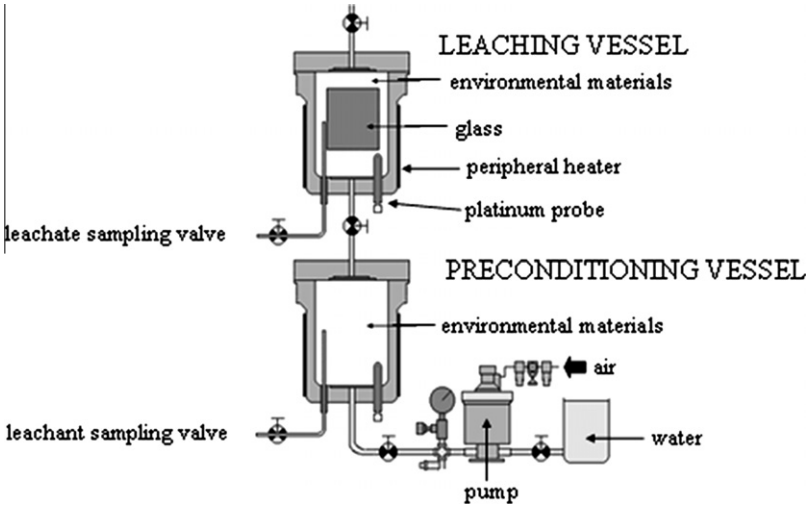

Fig. 1. Experimental setup of the long-term glass alteration process in a sand/granite environment.

Table 1
Nature and volume of environmental materials and water used for the 25.75 year-experiment in granite and sand. The volumes of the leaching water are those which have been experimentally measured before the experiment in a vessel filled with sand and granite.

	Leaching vessel		Preconditioning vessel	
	Nature	Total volume (cm^3)	Nature	Total volume (cm^3)
Leaching water	Solution from preconditioning vessel	330 (±10)	*Volvic* water	360 (±10)
Glass and environmental materials	SON68 glass	308	–	–
	Pieces of alloy	18	–	–
	Sand	806	Sand	833
	Pieces of granite	9	Granite	308

Table 2
Chemical composition of the SON68 glass (in mass percentages of oxide).

SiO_2	Al_2O_3	B_2O_3	Na_2O	CaO	ZnO	Li_2O	Fe_2O_3	P_2O_5	NiO	Cr_2O_3	ZrO_2	Cs_2O	SrO	Y_2O_3
45.48	4.91	14.02	9.86	4.04	2.50	1.98	2.91	0.28	0.74	0.51	2.65	1.42	0.33	0.20
MoO_3	MnO_2	CoO	Ag_2O	CdO	SnO_2	Sb_2O_3	TeO_2	BaO	La_2O_3	Ce_2O_3	Pr_2O_3	Nd_2O_3	UO_2	ThO_2
1.70	0.72	0.12	0.03	0.03	0.02	0.01	0.23	0.60	0.90	0.93	0.44	1.59	0.52	0.33

repository, and the alloy coupons simulated the canister. In the leaching vessel, the environmental materials were a mixture of granite (5%) and sand (95%). As the sand provided a high permeability, the solution was expected to quickly become homogeneous.

The preconditioning vessel was filled with natural French mineral water (*Volvic* water) to equilibrate it with the materials before this leachant solution comes in contact with the glass.

The two vessels were identical containers made of stainless steel. They were 142 (±1) mm high with an outer diameter of 100 (±1) mm and an internal volume of 1149 cm^3.

The glass cylinder was 7 cm in diameter and 8 cm high with a geometrical surface of 253 cm^2.

Each cell was heated using a "Vulcanic"-type circumferential heater, which maintained the temperature at 90 °C. The temperature inside each cell was checked using a platinum probe.

The pressure inside the cells was continuously maintained at 100 bar with a hydropneumatic pump. This pump was used to ensure watertightness by injecting water as soon as a sample had been collected. This system guaranteed that no gaseous phases were present in both vessels.

The inside of the vessels was covered with Teflon, and each vessel was equipped with a sampling valve which was fitted to a capillary sampling tube, which extends up to the center of the vessel, to a few millimeters from the glass surface. During the samplings, the solution removed from the preconditioning vessel was replaced with the same volume of *Volvic* water, and the solution removed from the leaching vessel was replaced with the same volume of solution from the preconditioning vessel.

The nature and volume of water, glass and environmental materials are given in the Table 1 for each vessel.

2.2. Composition of materials and water

The glass under study was SON68 glass whose theoretical composition is given in Table 2. This glass block is non-fractured.

The composition of the environmental materials is given in Table 3.

The granite came from a borehole performed in Auriat (France). For the preconditioning vessel, the granite came from a 6.3 cm-diameter core which was cut in order to obtain a height of 9.9 cm. This cylinder was then crushed until its granulometry was less than 5 mm. For the leaching vessel, the granite was cut into 36 samples of $5 \times 5 \times 10$ mm^3 each.

The sand was an industrial product (F25-type Silica and Kaolin) with a granulometry ranging between 0.1 and 0.63 mm and thus providing a porosity of 41%.

Table 3
Chemical composition of the granite and the sand (in mass percentages of oxide).

Mass%	SiO_2	Al_2O_3	CaO	MgO	Na_2O	K_2O	Fe_2O_3	TiO_2	P_2O_5
Granite from Auriat	72.4	13.7	0.9	1.0	3.6	4.8	1.8	0.24	0.20
F25 sand	⩾98.5	0.3–0.5	~0.1	~0.1	0.08		0.2	0.2	–

Table 4
Composition of *Volvic* mineral water contained in the 3 bottles used for the 25-year long experiment. Bottle 1 was used at the beginning of the experiment (in 1983), followed by bottle 2 (in 1997), and then bottle 3 (in 2007). These concentrations are those indicated on the bottles.

Species	Concentration of the different species ($mg\ L^{-1}$)		
	Bottle 1	Bottle 2	Bottle 3
SiO_2	23.0	30.0	31.7
Ca	9.8	9.9	11.5
Na	9.2	9.4	11.6
Mg	5.4	6.1	8.0
K	5.5	5.7	6.2
Mn	<0.002	–	–
Fe	<0.005	–	–
F	0.21	–	–
Cl	7.0	8.4	13.5
Sulphates	7.2	6.9	8.1
Bicarbonates	65.9	65.3	71.0
As	0.015	–	–
Pb	<0.005	–	–
Zn	<0.030	–	–
Cu	<0.002	–	–
Nitrates	1.0	6.3	6.3
Free CO_2	19.70	–	–
Characteristics	Bottle 1	Bottle 2	Bottle 3
Dry extract at 180 °C ($mg\ L^{-1}$)	116.6	109.0	130.0
pH	7.2	7.0	7.0
Conductivity at 25 °C (μS/cm)	162	–	–

The Hastelloy C4 alloy contained, in element percentages, 67.8% of Ni, 15.56% of Cr, 15.31 % of Mo, 0.78% of Fe, 0.27% of Ti, 0.22% of Co, and less than 1% of Mn, Si, P and S. This alloy was cut into parallelepipeds of $6 \times 8 \times 8\ mm^3$ each. These coupons were rinsed during 15 min in an ultrasonic bath with ethanol, and then with distilled water. Finally, in order to simulate the steel oxidation process in storage conditions, the pieces of Hastelloy C4 were placed in an aluminium oxide crucible to undergo a thermal treatment at 1000 °C during 1 h.

The composition of *Volvic* water (mineral water which comes from a granitic background) is given in Table 4.

At the beginning of the experiment and during the first 285 days, the valve between the two vessels was open. Thus, part of the soluble species from the leaching vessel diffused to the preconditioning vessel.

2.3. Setting-up of the experiment

The sand and granite were mixed together during 5 min. They were then introduced into the preconditioning vessel and slightly packed. The preconditioning vessel was closed and filled with *Volvic* water. We let the pump inject water until a few cm^3 of water overflowed from the vessel in order to remove all the residual air. The heating of the preconditioning vessel was started and the temperature reached 90 °C. The vessel was purged a second time and then the different valves were closed. The hydrostatic pressure was set at 100 bar. *Volvic* water was then preconditioned during 28 days at 90 °C and 100 bar, in contact with the environmental materials.

The leaching vessel was setup 28 days later. The sand, granite and Ni–Cr–Mo alloy were mixed together, and then a 30-mm thick layer was positioned at the bottom of the vessel and slightly packed. The glass was placed on the sand, in the center of the leaching vessel. The sampling tube was placed at about 2 mm from the surface of the glass. The empty space between the glass and vessel was then filled with the mixed materials. Then, the solution from the preconditioning vessel was injected into the leaching vessel. The temperature was set at 90 °C and the pressure at 100 bar.

2.4. Solution samplings: pH measurements and analysis

Samplings were performed in both vessels every 56 days using the sampling valves. During the first 47 months, 18 cm^3 were sampled each time. After this period, samples were reduced to 12 cm^3 until the end of the experiment. Based on the second volume, the collection of samples from the leaching vessel generated a low renewal rate of the solution of about 22% per year.

The pH of each sample was measured, firstly at about 80 °C immediately after it had been collected, and later on at room temperature.

After the pH measurements, 1 cm^3 of HNO_3 (normapur 65%) was added in all the samples. The samples were analyzed by Inductively Coupled Plasma (ICP-AES or ICP-MS) for Si, B, Al, Na, Sr, U, Th, Ce, and by Atomic Absorption Spectroscopy for Cs at the beginning of the experiment. Li, Mo, Ca, Zn, Fe, Zr, Nd were also quantified by ICP in the samples after 36 months. Mg and K were quantified after 79 months by ICP and Atomic Absorption Spectroscopy, respectively.

2.5. Calculation of the NL(B), Ee(B) and alteration rate

As the valve between the two vessels was open at the beginning of the experiment, part of the soluble species moved from one vessel to the other. Consequently, the calculation of the normalized boron mass loss (NL(B)) takes into account, on the one hand, the boron from the glass leaching (into the leaching vessel), and on the other hand, the boron which was measured in the preconditioning vessel:

$$\mathrm{NL(B)} = \frac{\left[\left(C_n^L \times V^L\right) + \left(C_n^C \times V^C\right) + \left(\sum_{i=1}^{i=n-1} C_i^L \times v\right) + \left(\sum_{i=1}^{i=n-1} C_i^C \times v\right)\right]}{x_B \times S_0} \quad (1)$$

C is the boron concentration in the sample (mg/L), subscript n or i represents time and superscript L or C represents the leaching vessel or the preconditioning vessel, respectively. V_L and V_C are the volumes of the leaching vessel and preconditioning vessel, respectively (L). v is the volume of the samples (L). x_B is the mass of the boron fraction inside the glass and S_0 represents its geometrical surface (cm^2).

Volumes V_L and V_C were determined before the 25.75 year-experiment. V_C was determined with a vessel which was filled with sand and granite in the same proportions as for the experiment, and V_L with a vessel which contained a block (representing the glass block) and which was then filled with sand and granite. V_C and V_L amounted to 360 cm^3 and 330 cm^3, respectively.

The equivalent thickness of altered glass is deduced from the normalized boron mass loss and depends of the glass density (ρ = 2.75 g cm^{-3}):

$$\mathrm{Ee(B)} = \frac{\mathrm{NL(B)}}{\rho} \quad (2)$$

As the glass block is cylindrical, the Ee(B) calculation must consider its curved shape. However, the glass block is big enough to be approximated as a flat surface, and thus Eq. (2) can be used.

The relative uncertainty on NL(B) is estimated at 30% by taking into account the highest uncertainty on the concentration and the highest uncertainty on the volume, and by ignoring the uncertainty on x_B. The relative uncertainty on Ee(B) is also estimated at 30% as the uncertainty on ρ is ignored.

Using the calculated Ee(B), the alteration rate can generally be calculated with Eqs. (3) and (3′) when Ee(B) has a linear trend over time:

$$r = \frac{d\mathrm{Ee(B)}}{dt} \tag{3}$$

$$r = \rho \times \frac{\mathrm{Ee(B)}}{t} \tag{3'}$$

The alteration rate is calculated with Eq. (4) using the mean measured thickness ($\bar{e}$, in μm) because the $\bar{e}$ value is not known when $\bar{e}$ begins to have a linear trend over time. This rate is the mean rate for the overall glass block during the 25.75 years:

$$\bar{r} = \rho \times \frac{\bar{e}}{t} \tag{4}$$

2.6. End of the experiment

To preserve the glass/alteration product interface, it was decided to stop the experiment without immediately removing the glass block from the vessel. Moreover, the altered glass surface/external medium interface was also preserved in order to observe any potential influence of the surrounding materials on the behavior of the glass. To do so, a careful stopping procedure was applied for the experiment, including freezing the whole reactor before drying the glass + environmental materials and embedding the overall system in a resin.

The experiment was to be ended when the samplings were to be performed, i.e. 56 days after the previous samplings. At that date, the heating of the leaching vessel was stopped and the valve between the two vessels was closed.

For the last sampling, five samples of solution were collected. The cap of the leaching vessel was opened and the first sample of about 3 cm^3 of solution was collected above the top of the glass block. Then, about 3 cm^3 were collected at three locations in the center of the vessel, i.e. on the opposite side of the capillary sampling tube, by the capillary sampling tube and at an angle of about 90° from the tube (and from its opposite side) (see Fig. 2).

Then, the cap of the leaching vessel was closed and the temperature probe was removed. The vessel was removed and a fifth sample of solution (about 3 cm^3) was collected below the glass block. To do so, it was necessary to move the liquid with a piston which was placed at the top of the leaching vessel.

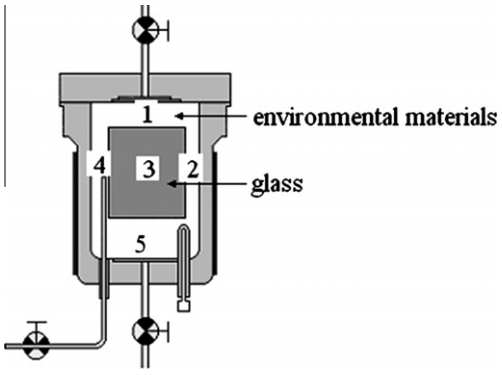

Fig. 2. Experimental setup for the collection of five samples of solution at the end of the 25.75 year-experiment.

The five samples of solution were filtered on membranes with a 0.45-μm pore size. Their pH was measured at room temperature. They were analyzed by ICP-AES to determine the concentration of B, Si, Na, Li, Mo, Al, Ca and Mg.

The system had to be transferred into a plastic vessel. In order to facilitate this transfer without disrupting the environmental materials, the leaching vessel was firstly placed inside a freezer at −25 °C during about 22 h. Once the system had frozen, it could be transferred relatively easily into a plastic vessel made of Teflon. Only a small amount of sand, alloy and granite pieces fell and were not transferred.

The system was oven-cured at 50 °C during 75 h and then at 90 °C during 23 h. Then, the sand was compacted again.

The system was degassed under vacuum and then embedded in an epoxy resin. Then, the system was oven-dried at 40 °C during 24 h and at 60 °C during 4 days to let the resin polymerize.

The glass block was cut into samples. Each sample was embedded in a resin, and then polished before being observed by SEM. A first global observation was attempted on an entire glass section in order to examine the homogeneity of the alteration products all around the glass block.

The glass, surrounded by the environmental materials, was cut horizontally into two sections, referred to as the top section and the bottom section (see Fig. 6). The remainder of the glass was cut vertically into three other samples. During the cutting with a diamonded saw, due to the difference in hardness between the glass and the resin, constraints were generated inside the glass block. As a result, some fractures appeared in the glass, particularly in the core section, and some samples were broken.

In order to prevent damage due to cracking, we decided to embed all samples in a resin after cutting.

The top section was polished to grade 4000 with SiC paper. The others samples were polished to grade 1200 with diamond-coated paper.

The SEM analyses were firstly performed with a Zeiss Leo 1450VP for the thickness measurements of the glass alteration layer, using a Si(Li) detector (cooled by liquid nitrogen) or an Analyzer Drift Detector X-act, cooled by Peltier effect (from Oxford Instruments), at an accelerating voltage of 15 kV.

The top section had not been metalized before the SEM analyses, which were carried out under a low vacuum (15 Pa). The other samples, which were smaller, were metalized with carbon. As a result, the SEM analyses could be performed under a high vacuum and with a better working distance.

The SEM analyses were carried out by using a Zeiss Supra 55 for the element quantification by EDS in the different parts of the alteration layer. This FEG-SEM is equipped with a Silicon Drift Detector X-max, cooled by Peltier effect (from Oxford Instruments). The accelerating voltage was 15 kV.

Some analyses were made with a CAMECA microprobe SX100 equipped of five spectrometers for the element quantification by WDS. All elements can be quantified by WDS except for H and Li. Each element of the pristine glass is calibrated with a standard, for example the B concentration is calibrated with the boracite. The accelerating voltage is 12 kV and the current intensity is 10 nA. The analyzed surface is 45 μm^2 on the pristine glass and the gel, and it is 0.5 μm^2 on the secondary phases.

2.7. Calculation of the total volume of the alteration layer

The total volume of the alteration layer was determined, regarding the glass block, as eight sections of 10 mm high (h) and with a perimeter (p) of 219.9 mm so as to calculate the volume

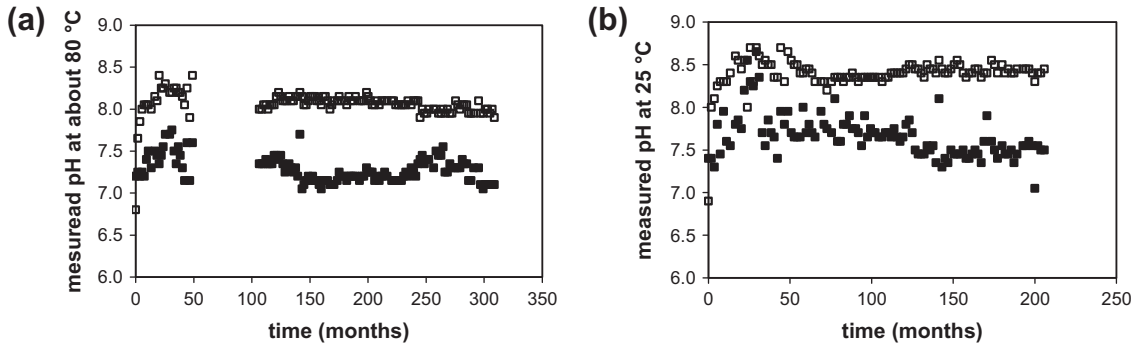

Fig. 3. pH measured at 80 °C (a) and at room temperature (b) in the preconditioning vessel (■) and in the leaching vessel (□). The variations for both pHs are shown as some pH values at about 80 °C have not been measured during 60 months, and as the pH has not been measured after 200 months at room temperature.

on the lateral part. This volume was added to the volume of the top base and the volume of the bottom base of the cylinder:

$$V = \left\{ \sum_{i=1}^{i=8} \bar{e}_i hp \right\} + (\bar{e}_u S) + (\bar{e}_d S) \quad (5)$$

$\bar{e}_i$ is the mean thickness of section i; $\bar{e}_u$ and $\bar{e}_d$ are the mean thicknesses of the top base and bottom base, respectively. S is the surface of one base of the cylinder.

3. Results

3.1. pH measurements

pH measurements are given in Fig. 3. The measurements performed continuously at 25 °C over 206 months vary between 7.3 and 8.5 in the preconditioning vessel during the first 100 months. Then, the pH becomes constant at 7.5 (at 25 °C) in the preconditioning vessel and at 8.5 in the leaching vessel. The measurements at about 80 °C show that the pH in the preconditioning vessel decreases slightly after 250 months.

3.2. Concentration variations

The concentrations of Si, B, Na, Mo, Li, Al, Ca and Mg in both vessels are specified in Fig. 4. At the beginning of the experiment, the concentrations in the preconditioning vessel are high as the valve between the vessels was open. Nine months later, this valve was closed. As a result, the concentrations in the vessel decrease and reach a constant value between 100 and 120 months later. This value is insignificant for B, Mo, Li and Al, but it amounts to 30 mg L^{-1} for Na, which is supplied by *Volvic* water (9 mg L^{-1}) and is released from the environmental materials (granite and sand) during the entire experiment.

In the leaching vessel, the Si and Li concentrations increase slightly as from 35 months until the end of the experiment, and the B, Na, Mo, Al concentrations decrease at the beginning (during 100 months). Concentrations then remain constant at about 32, 80, 6.5 for B, Na, Mo, respectively, and below 0.5 mg L^{-1} for Al. The Si, B, Na, Mo, Li concentrations in the leaching vessel are higher than the concentrations in the preconditioning vessel as these elements are mainly released during the glass dissolution process.

For Ca and Mg, concentrations are higher in the preconditioning vessel than in the leaching vessel (see Fig. 4). Both elements are significantly consumed in the leaching vessel during the glass dissolution process. Considering their concentrations in *Volvic* water, Mg is also consumed by the environmental materials, but Ca is released from the same materials.

Al concentrations are nearly similar in both vessels after 100 months (see Fig. 4). Conversely, K concentrations are scattered widely in the preconditioning vessel and in the leaching vessel during the experiment. K comes from *Volvic* water and probably from the environmental materials. However, the K concentration is probably not homogeneous, neither on a time basis nor a spatial basis, in both vessels.

3.3. Determination of the NL(B) and Ee(B)

The normalized boron mass loss is calculated with Eq. (1) after each sample has been collected from both vessels. Fig. 5 shows the general trend of NL(B) according to the alteration time.

During this experiment, boron is globally released from the glass at a rate of 6.10^{-3} g m^{-2} d^{-1} and the NL(B) reaches 77 (±24) g m^{-2} at the end of the experiment.

The equivalent thickness is calculated with Eq. (2). At the end of the experiment, the altered glass thickness is 28 (±9) μm.

3.4. Concentrations of different elements in the five locations

The pH measured in the leaching vessel, two months after the last sampling, is the same for the five solutions which were collected at five different locations (see Table 5).

The Si concentration is similar in each location, but it seems that there is a little more Si above than below the glass block (see Table 5).

Moreover, the B, Na, Li, and Mo concentrations are similar everywhere, except at an angle of 90° from the capillary sampling tube (in front of the glass block) where they are higher (6–12%). Thus, for these elements, the concentrations measured at the leachate sampling valve are representative of the concentrations measured in each location inside the leaching vessel, 56 days after the previous sampling campaign.

Al, Ca and Mg concentrations seem to be different in the five locations. For Al and Mg, these data are not necessary due to heterogeneities. As for Mg, the concentrations are too low. Concerning Al, we have noticed above that concentrations are very scattered in both vessels. Moreover, Al concentrations in the five locations are consistent with the Al concentrations measured at the sampling valve during the last 16 months of the experiment (0.03–0.19 mg/L). Therefore, there may only be heterogeneous concentrations of Ca in the leaching vessel 56 days after a sampling.

3.5. General characterization of the alteration film after the end of the experiment

In order to facilitate the representation of the zones analyzed by SEM, the glass block has been represented in the same configuration

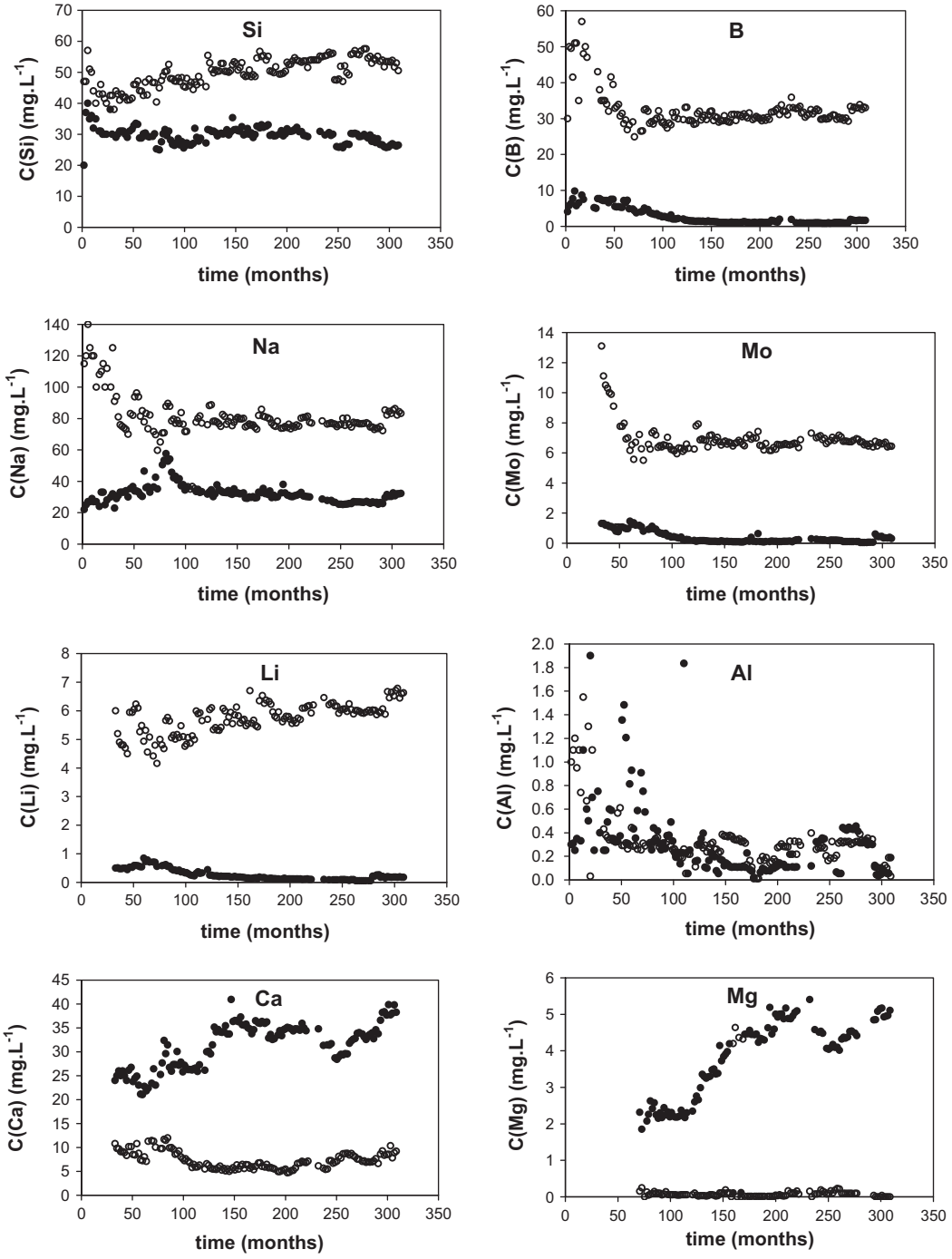

Fig. 4. Concentrations of Si, B, Na, Mo, Li, Al, Ca and Mg in the preconditioning vessel (●) and in the leaching vessel (○) determined by sampling the leachant and the leachate, respectively.

as in the leaching vessel in Fig. 6. The SEM analyses were performed at four levels and over six series of levels along the height (h) of the block, and in three zones on the periphery of the block.

The SEM analysis was initially performed on the entire upper section which was located at about 1 cm from the top of the glass block (in the leaching vessel). The observed alteration film contains a thin stripe (near the pristine glass) a thick gel and an outer layer (see Fig. 7B). The thin stripe cannot be analyzed as it is not thick enough for the SEM electron beam. The gel has a homogeneous chemical composition with a very little amount of Na and it is enriched with Si, Al, Ca and Zr compared to the composition of the pristine glass. The outer layer includes crystallized secondary phases contain P and rare earths like La, Ce, Nd, Pr, but no Na. In the top section, the thickness of the alteration film has two ranges of values: it is included between 2 and 3 μm or between 6 and 10 μm. The thickness decreases from 8 μm to 2 μm quite frequently. On the overall circumference of the top section, the pristine glass/gel limit is a linear front which is parallel to the gel/external medium interface.

As the glass alteration thickness is globally homogeneous in the entire top section with a mean value of 7.0 (±0.3) μm, the next samples, which correspond to a height-location of the glass cylinder, are only analyzed at two locations, i.e. near the sampling valve and further away from the valve.

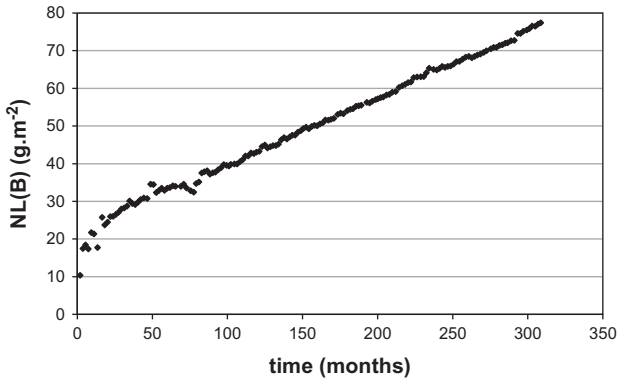

Fig. 5. Normalized boron mass loss, calculated with Eq. (1).

For the samples located at a height between 7 cm and 1 cm, the alteration film does not have a constant thickness. It is interesting to observe its different appearances in relation to the height (see Fig. 7). According to the height-location, the thickness and the morphology of the alteration layer are both heterogeneous.

The secondary phases do not seem to be present everywhere, especially in the upper half of the glass block.

In the lower half, the alteration layer has a much greater thickness and, for the most part, a non-linear front. In many locations, such as in the upper half, the gel has a homogeneous chemical composition, i.e. it is relatively enriched with Al, Ca and Zr in comparison to the pristine glass and it contains no Na. However, in the lower half of the glass block and at various locations, the gel has relatively different structures (see Fig. 7G, H and I) and includes some rounded shapes.

For all the samples, thickness measurements have been performed on a few SEM images with a 10-μm spacing between each measurement. The results are shown in Table 6. The thickness seems to increase near the sampling valve than farther away. However, the ratio between both values rarely exceeds 2 at the same height.

Moreover, the lower the location in the glass block, the thicker the alteration film. This trend is also illustrated in Fig. 8.

At $h = 0.5$ cm, the mean thickness near the sampling valve is 91.1 (±0.8) μm and it is 70.6 (±0.8) μm at 180° from the sampling valve. As opposed to the observation made previously on the top section, the thickness of the alteration layer is heterogeneous on the circumference of the cylindrical glass block in the lower half of the glass block.

At $h = 0$ cm, in the bottom base of the cylindrical block, the mean measured thickness is 74.3 (±0.5) μm, and at $h = 8$ cm, in the top base of the block, it is 6.5 (±0.3) μm.

We have observed, in the top section, that the pristine glass/gel limit is a linear shape parallel to the gel/external medium interface. On the contrary, most of the observed zones show a more or less irregular shape with peaks of gel which penetrate the glass (see Fig. 7).

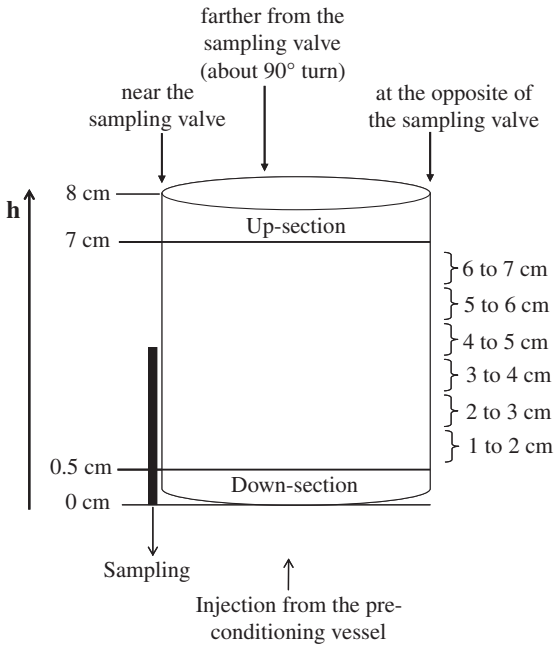

Fig. 6. Zones analyzed by SEM: various h values along the height (h) of the glass block and in three zones on the periphery.

3.6. Thickness measurements (SEM) of the alteration film versus the height-location on the glass block

As noticed above, the thickness of the alteration layer specifically depends of the height-location (h) on the glass block. In Fig. 8, it is assumed that the glass alteration is very different above and below the sampling valve (the sampling valve is at about $h = 4$ cm). In the upper half ($h > 4$ cm), the mean thickness is 6.7 (±0.3) μm. In the lower half ($h < 4$ cm), the significant thickness must be due to the renewal of the solution between the water injection point (below the lower base of the glass block) and the sampling valve. Thus, the thickness of the alteration layer reaches values which are about 10 times higher than the thickness of the upper half. The mean thickness in the lower half is 81.3 (±1.1) μm.

3.7. Estimation of the total volume of the alteration film

Eq. (5) was used to estimate the total volume of the alteration film at 1010 (±32) mm^3. The ratio of this volume to the geometrical surface of the glass block gives the mean thickness, i.e. 40 (±2) μm.

3.8. General elemental analyses (EDS)

In the upper half, the gel is very depleted in Na and enriched with Si, Al, Ca and Zr compared to the pristine glass. The secondary phases contain P and rare earths such as La, Ce, Nd and Pr.

Table 5
pH measured at room temperature and ICP concentrations (with uncertainties in brackets) for Si, B, Na, Li, Mo, Al, Ca and Mg just after the end of the 25.75 year-experiment.

Sample no.	pH	ICP concentrations in mg/L (and uncertainties)							
		Si	B	Na	Li	Mo	Al	Ca	Mg
1	8.25	52.64 (1.45)	32.74 (0.90)	83.11 (2.28)	6.45 (0.18)	6.37 (0.18)	0.12 (0.02)	7.55 (0.21)	<0.01
2	8.25	50.37 (1.38)	32.95 (0.90)	86.11 (2.36)	6.71 (0.18)	6.41 (0.18)	0.11 (0.02)	11.46 (0.31)	0.08 (0.02)
3	8.30	51.57 (1.43)	35.06 (0.97)	92.98 (2.58)	7.10 (0.20)	6.84 (0.19)	0.18 (0.03)	12.48 (0.35)	0.15 (0.03)
4	8.25	50.51 (1.42)	32.97 (0.93)	83.30 (2.34)	6.63 (0.19)	6.44 (0.18)	0.03 (0.01)	9.21 (0.26)	<0.01
5	8.25	49.58 (1.36)	32.74 (0.90)	84.52 (2.32)	6.58 (0.18)	6.39 (0.18)	0.02 (0.01)	9.25 (0.25)	0.13 (0.02)

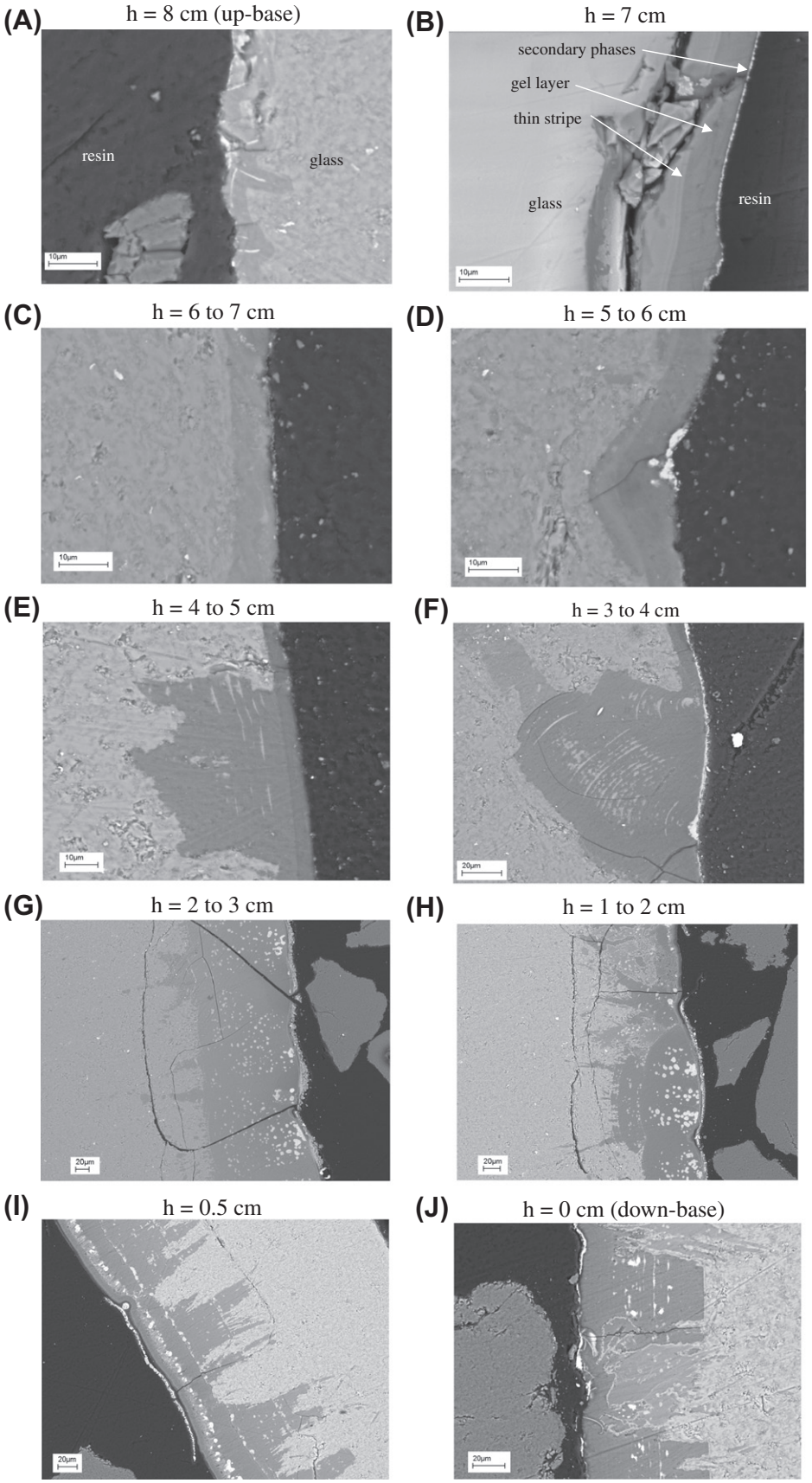

Fig. 7. SEM images of the pristine glass/alteration film interface for the glass block after 309 months of alteration. These images are shown according to the height (h) of the 8 cm-block. See Fig. 6 to see the location of the measurements.

Table 6
Mean measured thicknesses according to the height (h) of the 8 cm-block. The values in brackets are the uncertainties of the measured thicknesses. See Fig. 6 to know the location of the measurements.

h (cm)	Mean measured thickness (μm)	
	Near the sampling valve	Farther away from the sampling valve (about 90° turn)
6 to 7	8.1 (±0.2)	5.2 (±0.2)
5 to 6	8.1 (±0.3)	4.7 (±0.3)
4 to 5	13.4 (±0.3)	10.0 (±0.3)
3 to 4	44.6 (±0.9)	25.8 (±0.9)
2 to 3	121.1 (±1.1)	51.8 (±1.1)
1 to 2	90.4 (±1.1)	76.2 (±1.1)
0.5	91.1 (±0.8)	–

In the lower half, such as in the upper half, the gel is very depleted in Na but enriched with Al, Ca and Zr. However, it is depleted in Si. When the gel is very thick, it includes some rounded shapes (see Fig. 9A) which contain phosphorus and lanthanides (La, Ce, Pr, and Nd). In such locations, the precipitated phases are always comprised of Na, Mg, Zn and Ni, and sometimes of Mn. They seem to be clayey phases as they are in a sheet-type configuration (see Fig. 9B).

Moreover, at a height below 1 cm on the glass block, the secondary phases seem to be a mixture of phases containing Na, Mg, Zn, and Ni and phases containing lanthanide phosphates, as shown in Fig. 10.

3.9. Elemental analyses of magnesium

The EDS analyses performed on the lower half of the glass block show that magnesium is only present in the clayey phases, which have precipitated at the surface of the gel. These data were used to quantify Mg in these secondary phases at different heights on the glass block. As shown in Fig. 11A, the percentage of Mg in the secondary phases is negatively and linearly correlated to the distance from the bottom of the glass block.

Moreover, the composition of the secondary phases varies depending on the analysis location along the height of the glass block. However, the thickness of these phases seems to be proportional to the total thickness of the altered layer (see Fig. 11B). Both results confirm that Mg has a strong affinity with the clayey minerals precipitated at the interface between the gel and the solution.

3.10. Leaching of the environmental materials

From a general point of view, no environmental materials, or very few, seem to have been leached during the 25.75 year-experiment compared to the glass. Alteration products have rarely been observed (see below). However, such products can be ignored compared to the glass alteration products.

3.10.1. Ni–Cr–Mo alloy

The Hastelloy C4 alloy analyzed by SEM contains a large amount of oxygen (13.2%). However, the alloy had undergone a thermal treatment before the 25.75 year-experiment and has not been

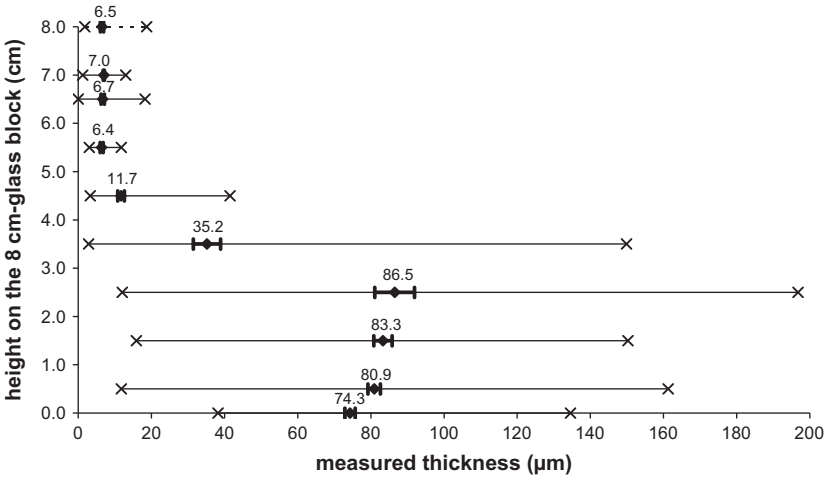

Fig. 8. Mean thicknesses measured along the height (h) of the 8 cm-block. The mean values are indicated above the corresponding point; the confidence intervals (at 90%) are represented by the thick solid lines; the ranges between the minimum value and the maximum value are represented by the dashed lines. The measurements made between 1 and 2 cm are considered, in this case, at 1.5 cm, and therefore for the six ranges specified in Table 6.

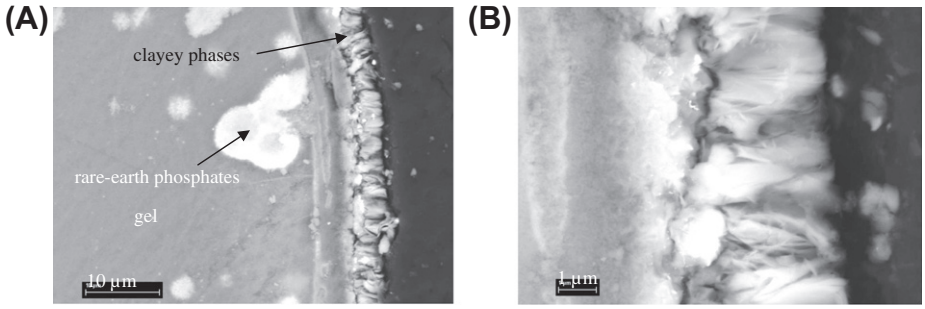

Fig. 9. SEM images of the alteration film; (A) gel with some rounded shapes and edged by some secondary phases; (B) zoom of these secondary phases.

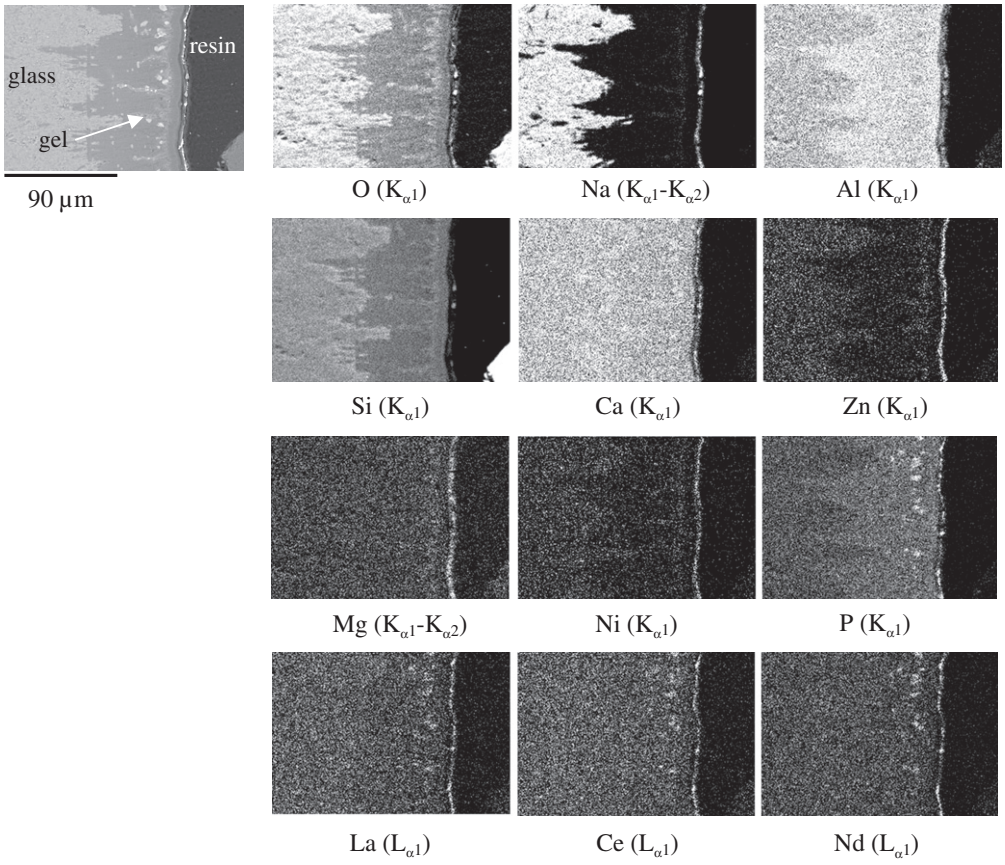

Fig. 10. EDS cartography of a very altered zone of the glass at a height below 1 cm on the glass block.

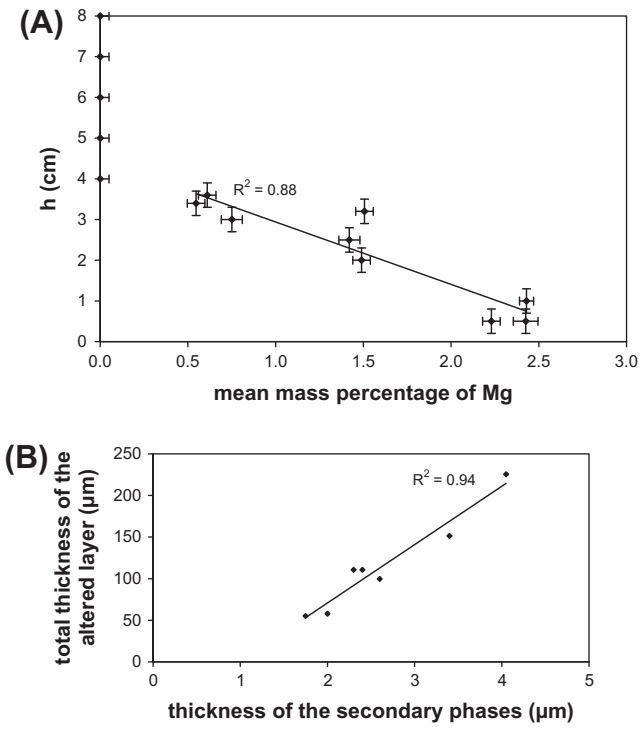

Fig. 11. Effect of magnesium in the lower half of the glass block. (A) Mean mass percentage of Mg, measured by EDS, in the secondary phases, along the height (h) of the 8 cm-block; the values at 0% for the upper half of the glass block mean that no Mg is detected by EDS/SEM; (B) thickness of the secondary phases according to the total thickness of the altered layer.

analyzed before the beginning of the experiment. Therefore, it is possible that it has not been oxidized during this experiment. Concerning the glass located near the alloy, it does not seem to be enriched with elements from the alloy. For example, the glass surface that is located in the vicinity of a piece of alloy does not include more Ni, Cr, and Mo (from the alloy) than the gel inside the glass that is located farther away from the alloy.

3.10.2. Granite

Two granite pieces have been analyzed by SEM. They include the characteristic phases of the granite from Auriat, i.e. quartz, plagioclase, microcline, biotite, apatite, zircon and a phase that has not been identified. Plagioclase has a oligoclase-like stœchiometry with a more or less depleted amount of Ca. Biotite is depleted in K and Si and enriched in Al. The analyzed apatite is a fluorapatite with a $Ca_5(PO_4)_3F_{1.8}$ stœchiometry, and the analyzed microcline has a $K_{0.9}Al_1Si_3O_{7.9}$ stœchiometry. Zircon is only present in small grains included in the other granitic phases (biotite or quartz). The last phase contains a large amount of Ca and lanthanides (La, Ce and Nd), and some Zr, Y and Th.

3.10.3. Sand

Sand does not seem to have been leached during the experiment. However, a few grains are entirely covered with an Fe oxide (or a mixture of Fe and Ti oxides).

Finally, in some rare cases, U has been adsorbed at the surface of a few sand grains with some Te, Ca and K.

3.11. WDS analyses of the glass block

The WDS analyses were performed to quantify all the elements present in the pristine glass as well as those present between the

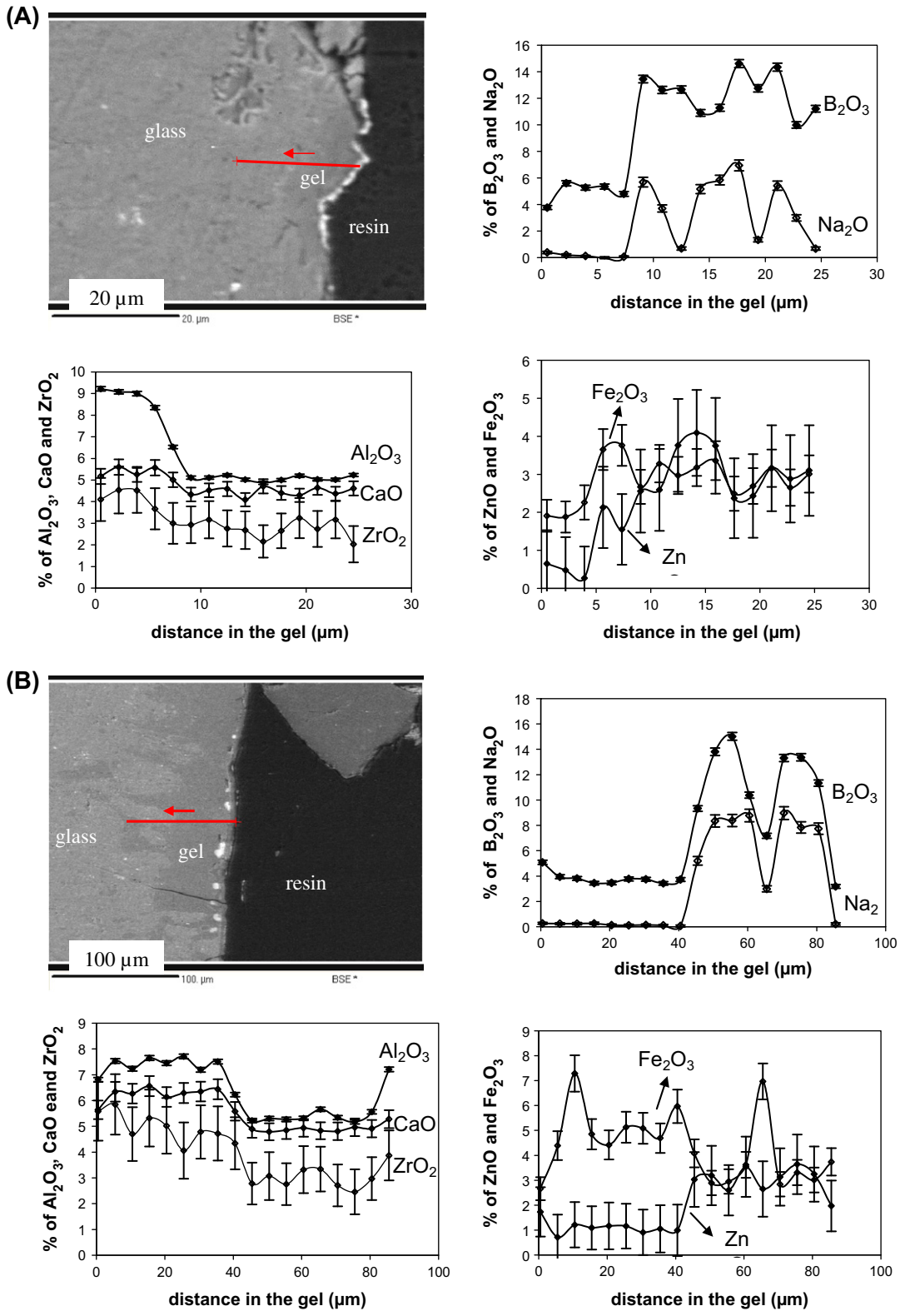

Fig. 12. Concentration of the main oxides of SON68 glass in the gel: (A) on a sample from the upper half of the glass block; (B) on a sample from the lower half.

edge of the gel and the pristine glass. Only H and Li are too light to be detected by WDS. Except for Li, all of the elements have been calibrated and then quantified in the pristine glass. The concentrations of most of the elements are consistent with the theoretical values determined for SON68 glass (see Table 2). The concentrations of B, Na, La and Nd have been slightly under-estimated, and the concentration of Si has been over-estimated (22.85 (±0.58)% by WDS for a theoretical value of 21.26 %). Moreover, for some elements (like Th and U), there is a very high uncertainty (with respect to the value). Finally, the sum of the concentrations of all the elements amounts to about 100% (between 96.7 and 101.6%).

In the upper half of the glass, one sample was analyzed to define a profile in the entire thickness of the gel (see Fig. 12A). The five first points are located in the gel and the others seem to be in the pristine glass, since the B_2O_3 concentration is close to 14.02% (the Na_2O concentration stays below its concentration in the pristine glass as this light element is labile under the electron beam). CaO and ZrO_2 concentration do not vary in the gel, but the Al_2O_3 concentration decreases from the edge of the gel to its bulk, and Fe_2O_3 and ZnO concentrations increase in the same direction.

In the lower half of the glass, the profile analyzed in the gel does not seem to finish in the pristine glass (see Fig. 12B), as the B_2O_3 concentration does not reach a plateau at about 14.02 %. However, the variations of the B_2O_3 concentration indicate the zones where the pristine glass is present, such as observed on the image. The concentrations of the main oxides are constant in the gel (for the first nine points), but the Fe_2O_3 concentration varies in the gel between 2.66 (±0.46) and 7.29 (±0.73)%.

Finally, the WDS analyses confirmed that most of the secondary phases are lanthanide phosphates. In one location, three points provided mean values of 5.26 (±0.25)% of La, 6.24 (±0.23)% of Ce, 6.36 (±0.15)% of Pr, 6.21 (±0.43)% of Nd, and 3.69 (±0.23)% of P.

4. Discussion

4.1. Concentrations of the different elements during the experiment

As the concentrations measured in the leaching vessel shown in Fig. 4 are almost always the same over 56 days (maximum) after sampling B, Na, Mo, Ca and Mg, and as Si and Li concentrations slightly increase in the vessel, the glass alteration process seems to have remained in a stable state during the 25.75 years: its alteration rate remained at a constant value.

The concentrations of elements depend on many parameters, i.e. their concentration in *Volvic* water, their possible release from environmental materials (granite and sand), glass dissolution and hydrodynamic transport processes, the injection of water from the preconditioning vessel, the position of the injection point and the sampling location.

Considering the composition of the environmental materials (see Table 3), it is believed that some elements may be released from such materials, i.e. Si, Na, Al, Ca, Mg, and K may be released from granite and sand, and Ni, Cr, and Mo from alloy.

Based on the concentration variations observed in both vessels (see Fig. 4) and the composition of *Volvic* water (see Table 4), it appears that Na and Ca are released from granite and sand. Na is also released from the glass. However, Ca is globally consumed in the leaching vessel, thus it is retained in the alteration layer of the glass. Moreover, Mg is consumed by the environmental materials as the concentrations measured in the preconditioning vessel (2 mg L^{-1} between 70 and 120 months) are lower than the Mg concentration in *Volvic* water (5.4 mg L^{-1} in the first bottle). In the leaching vessel, Mg is likely to be retained by the environmental materials, but it also seems to be consumed during the glass alteration process as the measured concentrations are very low (less than 0.2 mg L^{-1}).

B and Li are only released from the glass, but Li is partially retained in the gel layer. Eq. (1) can be applied to Li to calculate its retention factor:

$$R(i) = 1 - \frac{NL(i)}{NL(B)} \quad (5)$$

After 40 months, *R*(Li) amounts to 70% and decreases down to 30% at the end of the experiment. It appears that Li is less and less retained in the gel.

The retention factors for Mo also decrease during the experiment until reaching a plateau at 33% after 257 months. As *R*(Mo) and *R*(Li) have a similar trend, it seems that Mo is not released from the alloy.

Table 7
Comparison of the retention of Si and Mo with the results from the study of Curti et al. [50] who have performed calculations with Li as the normalized element for SON68 glass leaching in pure water at 90 °C.

	Curti et al. [50]		Current study		
Time (y)	5.7	12.2	5.75	12.25	25.75
R(Mo) (%)	47.7	52.8	48.2	40.6	32.6
R(Si) (%)	76.6	79.8	72.2	70.1	69.6

The retention factors for Mo and Si can be compared with those of the Curti's study conducted in static mode and with initially pure water [50], although Si is also supplied by all the environmental materials present in our study. First, their values are higher as Li has been considered as the normalized element for calculating the retention factors (see Table 7). Moreover, the retention factors for Mo and Si obtained in pure water increase from 5.7 to 12.2 years. Those differences could be due to the experimental condition: static mode, atmospheric pressure, low S/V ratio for the Curti's experiment, or to the presence of sand and granite in our experiment. At this stage, it is impossible to decide. Further reactive/transport simulations will help us to identify the reason of this difference.

4.2. Concentrations of the different elements at the end of the experiment

The concentrations measured at the end of the experiment at five locations inside the leaching vessel (see Table 5) show that the elements released from the glass (B, Na, Li, and Mo) have similar concentrations in the five locations, except for location no. 3 (at an angle of about 90° from the sampling valve). The concentrations of these elements remain homogeneous in the leaching vessel 56 days after sampling. For these elements, the concentration measured at the sampling valve for the entire duration of the experiment can be considered as representative of a homogeneous concentration in the entire vessel.

The Si concentration is almost the same in each location considering the uncertainties. However, the Si concentration is slightly higher above the glass block (sample no. 1) than below (sample no. 5) (see Table 5). This trend is consistent with the reduced alteration of the glass in its top section.

However, the B concentrations do not confirm this fact as they are similar above and below the glass block.

The water flow is a key factor as the renewal of the solution contributes to increasing the glass dissolution rate [38]. Thus, it is necessary to understand the hydrodynamic transport process inside the leaching vessel. As many elements are present in the glass and in the environmental materials, finding a hydrodynamic tracer in the leaching vessel is difficult. Only Mg and K could be used as hydrodynamic tracers because they are the only elements which come only from the environmental materials. However, as mentioned above, Mg is consumed by the materials and during the glass dissolution process. As a result, Mg cannot be used as tracer for the hydrodynamic transport process. As for K, its concentrations have not been measured at the five locations at the end of the experiment and its concentration values in both vessels are very scattered (not shown in Fig. 4).

Therefore, no element can be used as a hydrodynamic transport tracer.

4.3. Comparison of the calculated and measured thicknesses

The thickness of the altered glass has been calculated with the equivalent boron mass loss and it amounts to 28 (±9) μm. The

alteration film thickness has been determined with 3122 measurements and its mean value is 40 (±2) μm. However, this value may be slightly over-estimated as it takes into account the entire thickness of the alteration layer comprising the gel and the secondary phases. Moreover, it is not always easy to measure the alteration film, as there are some irregular shapes at the glass/gel interface and sometimes some shapes of gel which are included inside a zone of pristine glass.

It is generally assumed that the glass transforms into a gel with a constant volume [18,21]. Thus, it seems that for this 25.75 year-experiment, such as for experiments conducted over a shorter period, and the glass dissolution was isovolumetric.

Moreover, in our experiment, there is no dissolution of the gel such as for the alteration of glass in contact with clay [25]. Therefore, the gel must not dissolve during the 25.75 years since the mean measured thickness is not actually lower than the equivalent boron mass loss.

4.4. Glass leaching kinetics

4.4.1. Water renewal effect

During the 25.75 year-experiment, the surface flow rate amounted to 7.9×10^{-6} m d^{-1}, and the mean alteration rate to 6×10^{-3} g m^{-2} d^{-1}. These values have been compared to those obtained in pure water at 90 °C with SON68 glass [38]. The point represented with an open circle in the middle of the solid segment in Fig. 13 was determined with the normalized boron mass loss and is consistent with the measured alteration rate for different flow rates of pure water. During the 25.75 year-experiment, the alteration rate seems to be mainly due to a flow rate effect.

The rate measured for the 25.75 year-experiment is a mean rate, assuming that the alteration is homogeneous on the overall glass block. However, SEM observations of the glass block have shown that the alteration is very heterogeneous between the upper half and the lower half of the block. As the alteration rate is about 10 times higher in the lower half, it has also been calculated with Eq. (4) where, in the first calculation, $\bar{e}$ is the mean thickness measured in the lower half (81.3 μm) and, in the second calculation, $\bar{e}$ is the mean thickness in the upper half (6.7 μm). Thus, alteration rates range from 2.0×10^{-3} g m^{-2} d^{-1} to 24.1×10^{-3} g m^{-2} d^{-1} and are represented by the solid segment in Fig. 13. As the open circle is approximately in the middle of the alteration rate range, these data confirm that the glass dissolution was isovolumetric during the 25.75 years.

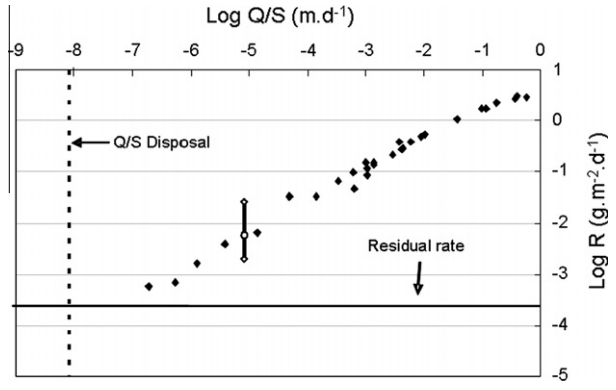

Fig. 13. Variation of the alteration rate (R) of SON68 glass measured according to the surface flow rate (continuous flow), in pure water at 90 °C [38]. The solid line represents the residual rate reached in pure water in a closed system, and the dashed line represents the flow rate expected in the French disposal concept. Concerning the 25.75-year experiment, the point with open circle (in the middle of the solid segment) corresponds to the alteration rate calculated with the NL(B) (Eq. (3′)), and the solid segment corresponds to the range of alteration rates considering the highest alteration rate (calculated with the mean thickness measured in the lower half of the glass block in Eq. (4)) and the lowest alteration rate (calculated with the mean thickness measured in the upper half of the glass block in Eq. (4)).

The alteration rate measured in our experiment seems to be mainly due to a flow rate effect. However, the conditions of the experiments, which are carried out with a continuous flow rate of pure water, are not really similar to the conditions of the 25.75 year-experiment, since the flow is generated by the brief samplings and the solution supplies reactive elements such as Mg.

As the thickness of the altered glass is much higher in the lower half than in the upper half, it appears that the alteration greatly depends on the local supply of elements and on the local flow rate.

Concerning the flow rate, it is likely that an anisotropic water flow has been generated in the lower half of the leaching vessel due to the solution injected at the bottom of the vessel and to the samples collected in center of the vessel. However, this has not been proved. This hypothesis would be consistent with the trend shown in Fig. 8, in which it is assumed that glass alteration is greater in the presence of a flow rate. For our experiment, the flow rate must be considered locally in the leaching vessel.

The quantification of the actual flow rate will be the subject of a future study in aim of improving our understanding of the coupling between hydrodynamics and chemistry.

4.4.2. Effect of the environmental materials

The few pieces of environmental materials which have been observed by SEM do not include very leached or damaged parts and do not have high concentrations of the elements released from the glass. Three specific observations have been made: (1) the presence of a non-identified phase which is included in the granite and which contains some lanthanides (La, Ce, and Nd), Zr, Y and Th; (2) the presence on a few sand grains of iron (and titanium) oxides that seem to cover the entire surface of the sand grain; (3) the presence of U (more than 30%), and some Te, Ca and K at the surface of rare sand grains.

All these elements could be due to the glass leaching process. However, with these data, it is difficult to assume that the environmental materials have played a role in the leaching kinetics of the glass.

The Auriat granite used in this study is mainly comprised of several primary minerals, i.e. quartz (30–37%), plagioclase (29–34%), microcline (18–25%), biotite (7–11%) and muscovite (0–6%), and also contains apatite, zircon, sphene, monazite and rutile [51,52]. The plagioclase from this granite has an oligoclase-type composition. Moreover, the composition of the granite regarding rare-earth elements (La and Ce) is determined by the depth at which the granite sample has been collected [49].

A hydrothermal alteration of the granite causes of the transformation of the biotite mainly into chlorite, and causes of an alteration of the calcic part of the plagioclase [51–53].

In our study, we have also observed the alteration of biotite and the alteration of the calcic part of oligoclase (anorthite). Biotite is depleted in K and Si and enriched in Al, and oligoclase is more or less depleted in Ca. Following the experiment, the granite includes the following minerals: quartz, altered oligoclase, microcline, altered biotite, apatite, zircon, and a phase bearing lanthanides, Zr, Y and Th. The SEM observations performed on two pieces of granite have not enabled to identify any muscovite.

4.5. Distribution of the elements in the gel

The EDS and WDS analyses revealed that the gel is enriched in Al, Ca, Zr and that the most secondary phases are lanthanide phosphates.

With the analyses of the gel (by WDS), we can see that Fe concentrations are relatively variable in most cases. Moreover, Al and

Zn concentrations seem to vary in a quite thin gel, but are constant in a thick gel (observed in a sample from the lower half of the glass block – see Fig. 12B). Ca and Zr concentrations are likely to always be constant in the entire thickness of the gel.

4.6. Secondary phases

The secondary phases that are formed on borosilicate glasses are mainly lanthanide phosphates [20] or phyllosilicates [21,54,55]. Phyllosilicates can bear Zn, Ni, Mn and Fe [50] at higher concentrations than in the glass (in absence of Mg). Moreover, Zn and Ni are likely to increase the glass dissolution rate with the formation of trioctahedral smectites such as sauconite in the presence of Zn or pimelite in the presence of Ni [22].

Rare-earth phosphates have been observed in many studies [39,50,56–58] due to the fact that rare-earth ions have a low solubility and that phosphate ions form stable complexes with lanthanides [59,60]. A recent study shows that La has such a high affinity for P that lanthanum phosphate forms when the P/Si atomic ratio of the glass is only 1/20 [58].

In our study, the main secondary phases that have been formed are lanthanide phosphates. They have mostly precipitated at the gel/solution interface. However, in a thick gel, they mainly tend to precipitate and form rounded shapes inside the gel. In this last case, the Mg from the leachant solution is involved in the formation of the secondary phases at the gel/solution interface. This observation allows asking us if the formation of Mg-clayey phases is partly involved in the formation of rare-earth phosphates precipitated inside the gel.

4.7. Location of U and Th

Th has a similar behavior to that of the lanthanides [56] as it is retained inside the gel by coprecipitation. In our study, Th concentrations in the samples are lower than the quantification limit of the ICP as this element is not very soluble. The alteration layer of the glass seems to be enriched in Th.

Concerning U which is released from the glass, it is likely to be mainly precipitated in the surface layer [37]. However, U can form some uranyl silicate phases and uranyl oxide hydrates under oxidizing conditions [61]. In our study, the U concentrations in the solution are scattered in both vessels and vary between 0.005 and 0.2 mg L^{-1}: U can be present in the solution as uranyl silicate. This datum could explain the presence of U adsorbed on some sand grains.

4.8. Effect of magnesium

Magnesium is an element which has attracted our attention, as it is present in the secondary phases but does not come from the glass. Magnesium is mainly supplied by *Volvic* water and enters the leaching vessel with the solution from the preconditioning vessel in concentrations between 2 and 5 mg L^{-1}. Magnesium can take part in the formation of phases which, according to experiments conducted with Mg-doped glass, highly enhance its alteration [30,49,50].

The alteration rate of SON68 glass (without Mg) is smaller than that of MW glass which contains Mg [50] – the alteration rate is 1.3 (±0.2) × 10^{-4} g m^{-2} d^{-1} for SON68 and 9.6 (±5.3) × 10^{-4} g m^{-2} d^{-1} for MW. In the case of MW glass, Mg is included in the alteration products, such as clays, which catalyze the glass dissolution reaction. The characterized phase has a composition which is halfway between that of hectorite, saponite and montmorillonite [50] and is a crystalline silicated phase incorporating Mg and Ni simultaneously [62].

As for the magnesium supplied by the glass, the magnesium from groundwater can contribute to emphasizing the glass dissolution process. When in contact with an Mg-rich solution, smectite phases have also been observed on AVM glass [23]; a structural analysis has enabled to identify Mg-smectites, whose composition is halfway between that of hectorite and saponite. Moreover, Abdelouas et al. [37] have noticed that Mg enhances the precipitation of magnesium clays with the forming elements of the glass network (Si and Al) to form a saponite-type clay.

More recently, Frugier et al. [30] have also observed this phenomenon on an AVM glass bearing Mg and leached in pure water: after their experiment, the Mg is retained in the crystallized secondary phases which supply some Si and Al. As Si and Al can contribute to form the gel, the formation of phyllosilicates rich in Mg leads to the persistence of the high dissolution rate [30].

Based on all the previous data collected to discuss our study, it is likely that the secondary phases observed in the lower half of the glass block are clayey phases containing magnesium that have precipitated with the Mg from the leachant solution of the preconditioning vessel. The secondary phases bearing Mg, Ni and Zn, which have formed, may be (Ni, Zn)-hectorite or (Ni, Zn)-montmorillonite.

Thus, magnesium from the solution may contribute to the formation of Mg-clays with the silicon of the gel. In such a case, the passivating effect of the gel decreases [18], leading to an enhanced dissolution, and then to an increased thickness of the altered layer. The Mg reactivity hypothesis is confirmed by the significant glass alteration observed in the lower half of the glass block, in comparison to the upper half, in which the alteration is less significant and the alteration products do not contain any magnesium.

This is supported by the observation reported on Fig. 11A showing a magnesium enrichment in the phyllosilicate phases that clearly increases as *h* diminishes. However, these phyllosilicates have a much lower density than the pristine glass, and can have a variable density according to their location. The depth of the SEM electron beam must be different for each analysis performed on the phyllosilicates, and, as result, the Mg quantification may not be reliable.

Moreover, the thickness of the magnesium phases is directly linked to the total thickness of the altered film (cf. Fig. 11B). These data seem to prove that the magnesium contribution of the solution may control the thickness of the secondary clayey phases, and thus the total thickness of the altered layer. Therefore, the secondary phases containing magnesium could be due to the magnesium contribution of the solution from the preconditioning vessel and of the hydrodynamic transport in the leaching vessel.

Although Mg can enhance the glass dissolution as we have shown it above, it is important to remind that it can also reduce the glass dissolution rate in some conditions, probably when it is incorporated in the gel rather than in secondary crystalline phases [63–65].

5. Conclusions

Solid characterization provided unexpected results whereas leaching data provided a very constant glass dissolution rate, which was quite close to the rate measured in slowly renewed pure water. In the present integrated experiment of a mockup simulating glass alteration in an open granitic environment, the thickness of the alteration layer is not at all homogeneous on the overall glass block. The alteration layer is much thicker in the lower half of the glass block which was near the injection point of the solution coming from the preconditioning vessel. Thus, the hydrodynamic transport of the soluble species must be a key factor for the local glass alteration process.

However, Mg seems also to play a major role in the increase of the glass dissolution rate in the lower half of the glass block, since the secondary phases are Mg-rich phyllosilicates in this area.

Moreover, the environmental materials are not really altered. Thus, the two mean factors controlling the glass dissolution rate during this 25.75-year experiment are at the first order the hydrodynamic transport process and secondly the local chemistry of the solution with the specific contribution of Mg. Considering that the local flow rate and the local chemistry are different in every place around the glass block, the thickness of the alteration layer vary with a factor about 10 on the glass block after a 25.75 year-alteration. Thus, in contact with water during more than 1000 years and in a granitic environment, the SON68 glass will have an alteration layer whose thickness could be very variable.

But, in the French disposal concept, the presence of clay instead of granite and the flow rate which is very much slower than in this current study (see Fig. 13) do not allow us to know the behavior of the glass in these conditions. However, thanks to this study, we can assume that, in the storage conditions in a clayey environment, the main factor controlling the glass dissolution rate would be the water renewal rate near the glass surface. This factor will directly influence the chemistry of the solution and then the glass reactivity.

In order (i) to maximize our understanding of this experiment and (ii) to assess the implication of such results on the long-term behavior of HLW glass in geological disposal conditions, we plan to implement a simulation by coupling a chemistry model of the glass alteration process (the GRAAL model [6,16]) with a hydrodynamic model. First and foremost, it is necessary to define the hydrodynamic parameters of the transport process in the leaching vessel considering spatial and time parameters.

Acknowledgements

The authors are very grateful to Emmanuelle Brackx and Alexis Chocard for the microprobe and SEM analyses, respectively. They would also like to thank Catherine Fucili, Mathilde Bonnehorgne and Barbara Deschamps. The authors thank also the anonymous reviewer for his remarks which have allowed us to improve this manuscript.

References

[1] ANDRA, 2005. Evaluation of the feasibility of a geological repository in an argillaceous formation. Andra report available on <http://www.andra.fr>.
[2] N. Godon, Z. Andriambololona, J.P. Mestre, E. Vernaz, P. Müller, M. Schvoerer, N. Jacquet-Francillon, Part A: Radioactive SON681817L1C2A2Z1 glass interaction with environmental materials, Nuclear Science and Technology (1990) Commission of the European Communities.
[3] T. Ohe, M. Tsukamoto, J At Energy Soc Jpn 33 (1991) 761–770.
[4] J.P. Glatz, E.H. Toscano, G. Pagliosa, A. Nicholl, J. Nucl. Mat. 223 (1995) 84–89.
[5] G.G. Wicks, J. Nucl. Mat. 298 (2001) 78–85.
[6] P. Frugier, S. Gin, Y. Minet, T. Chave, B. Bonin, N. Godon, J.E. Lartigue, P. Jollivet, A. Ayral, L. De Windt, G. Santarini, J. Nucl. Mat. 380 (2008) 8–21.
[7] B.C. Bunker, J. Non-Cryst. Solids 179 (1994) 300–308.
[8] R.H. Doremus, J. Non-Cryst. Solids 19 (1975) 137–144.
[9] W.A. Lanford, K. Davis, P. Lamarche, T. Laursen, R. Groleau, J. Non-Cryst. Solids 33 (1979) 249–266.
[10] G. Geneste, F. Bouyer, S. Gin, J. Non-Cryst. Solids 352 (2006) 3147–3152.
[11] L.L. Hench, D.E. Clark, J. Non-Cryst. Solids 28 (1978) 83–105.
[12] J.L. Noguès, Les mécanismes de corrosion des verres de confinement des produits de fission, Thesis (1984), Sciences et Techniques du Languedoc.
[13] C. Jégou, S. Gin, F. Larché, J. Nucl. Mat. 280 (2000) 216–229.
[14] S. Gin, Protective effect of the alteration gel: a key mechanism in the long-term behavior of nuclear waste glass, in: K. Hart, G.R. Lumpkin (Eds.), Scientific Basis for Nuclear Waste Management XXIV, Mat. Res. Soc., Sydney, 2001, pp. 207–216.
[15] C. Cailleteau, F. Angéli, F. Devreux, S. Gin, J. Jestin, P. Jollivet, O. Spalla, Nat. Mater. 7 (2008) 978–983.
[16] P. Frugier, T. Chave, S. Gin, J.E. Lartigue, J. Nucl. Mat. 392 (2009) 552–567.
[17] E. Vernaz, S. Gin, C. Jégou, I. Ribet, J. Nucl. Mat. 298 (2001) 27–36.
[18] S. Gin, I. Ribet, M. Couillard, J. Nucl. Mat. 298 (2001) 1–10.
[19] T.A. Abrajano, J.K. Bates, A.B. Woodland, J.P. Bradley, W.L. Bourcier, Clay Clay Mineral. 38 (1990) 537–548.
[20] J.L. Noguès, E. Vernaz, N. Jacquet-Francillon, Nuclear glass corrosion mechanisms applied to the French LWR reference glass, in: C.M. Jantzen, J.A. Stone, R.C. Ewing (Eds.), Scientific Basis for Nuclear Waste Management VIII, Mat. Res. Soc., Pittsburg, PA, 1985, pp. 89–98.
[21] N. Donzel, S. Gin, F. Augereau, M. Ramonda, J. Nucl. Mat. 317 (2003) 83–92.
[22] T. Chave, Etude des mécanismes d'altération par l'eau du verre R7T7 en milieu confiné, compréhension et modélisation de la cinétique résiduelle, Thesis (2008), Université Montpellier II, Sciences et Techniques du Languedoc.
[23] B. Thien, N. Godon, F. Hubert, F. Angéli, S. Gin, A. Ayral, Appl. Clay Sci. 49 (2010) 135–141.
[24] B.E. Scheetz, W.P. Freeborn, D.K. Smith, C. Anderson, M. Zolensky, W.B. White, The role of boron in monitoring the leaching of borosilicate glass waste forms, in: C.M. Jantzen, J.A. Stone, R.C. Ewing (Eds.), Scientific Basis for Nuclear Waste Management VIII, Mat. Res. Soc., Pittsburg, PA, 1985, pp. 129–134.
[25] I. Ribet, S. Gin, N. Godon, P. Jollivet, Y. Minet, B. Grambow, A. Abdelouas, K. Ferrand, K. Lemmens, M. Aertsens, V. Pirlet, D. Jacques, J.L. Crovisier, G. Aouad, A. Arth, A. Clément, B. Fritz, G. Morvan, I. Munier, M. Del Nero, A. Ozgümüs, E. Curti, B. Luckscheiter, B. Schwyn, GLASTAB, Long-term behaviour of glass: improving the glass source term and substantiating the basic hypotheses, Contract N FIKW-CT-2000-00007. European commission, 5th Euratom Framework Programme 1998-2002.
[26] S. Gin, Etude expérimentale de l'influence d'espèces aqueuses sur la cinétique de dissolution du verre nucléaire R7T7, Thesis (1994), Université de Poitiers.
[27] O. Ménard, Partage des terres rares et des actinides entre solution et produits d'altération du verre nucléaire type R7T7 en fonction des conditions de stockage, Thesis (1995), Université de droit, d'économie et des Sciences, Aix-Marseille.
[28] I. Tovena, Influence de la composition des verres nucléaires sur leur altérabilité, Thesis (1995), Université de Montpellier.
[29] S. Gin, C. Jégou, Limiting mechanisms of borosilicate glass alteration kinetics: Effect of glass composition, in: A.A. Balkema (Eds.), Water-Rock Interaction 1, Villasimius (Italy), 2001, pp. 279-282.
[30] P. Frugier, C. Martin, I. Ribet, T. Advocat, S. Gin, J. Nucl. Mat. 346 (2005) 194–207.
[31] F. Angeli, M. Gaillard, P. Jollivet, T. Charpentier, Geochim. Cosmochim. Acta 70 (2006) 2577–2590.
[32] N. Rajmohan, P. Frugier, S. Gin, Composition effects on synthetic glass alteration mechanisms (Part 1: Experiments), Chem. Geol., in press, doi:10.1016/j.chemgeo.2010.10.010.
[33] Z. Boksay, G. Bouquet, Phys. Chem. Glasses 21 (1980) 110–113.
[34] S. Gin, J.P. Mestre, J. Nucl. Mat. 295 (2001) 83–96.
[35] K.G. Knauss, W.L. Bourcier, K.D. McKeegan, C.I. Merzbacher, S.N. Nguyen, F.J. Ryerson, D.K. Smith, H.C. Weed, L. Newton, Dissolution kinetics of a simple analogue nuclear waste glass as a function of pH, time and temperature, in: V.M. Oversby, P.W. Brown (Eds.), Scientific Basis for Nuclear Waste Management XIII, Mat. Res. Soc., Pittsburg, PA, 1990, pp. 371–381.
[36] K. Lemmens, P. van Iseghem, The long-term dissolution behaviour of the Pamela borosilicate glass SM527 – Application of SA/V as accelerating parameter, in: C.G. Sombret (Ed.), Scientific Basis for Nuclear Waste Management XV, Mat. Res. Soc., Pittsburg, PA, 1992, pp. 49–56.
[37] A. Abdelouas, J.L. Crovisier, W. Lutze, B. Grambow, J.C. Dran, R. Müller, J. Nucl. Mat. 240 (1997) 100–111.
[38] S. Gin, I. Ribet, P. Frugier, T. Chave, F. Angeli, J.E. Lartigue, G. de Combarieu, N. Godon, Assessment of nuclear glass behavior in a geological disposal conditions: Current state of knowledge and recent advances, European Nuclear Conference, Versailles, 2005.
[39] S. Gin, C. Jégou, E. Vernaz, Appl. Geochem. 15 (2000) 1505–1525.
[40] T. Chave, P. Frugier, S. Gin, A. Ayral, Glass-water interphase reactivity with calcium rich solutions, submitted for publication.
[41] K. Lemmens, J. Nucl. Mat. 298 (2001) 11–18.
[42] S. Gin, P. Jollivet, J.P. Mestre, M. Jullien, C. Pozo, Appl. Geochem. 16 (2001) 861–881.
[43] L.L. Hench, L. Werme, A. Lodding, J. Nucl. Mat. 126 (1984) 226–233.
[44] H.P. Hermansson, H. Christensen, I.K. Björner, L. Werme, D.E. Clark, Nucl Chem Waste Manage 5 (1985) 315–332.
[45] H. Zhang, J.W. Yang, B.J. Li, S.G. Luo, Nucl. Sci. Tech. 17 (2006) 158–163.
[46] C.M. Jantzen, D.I. Kaplan, N.E. Bibler, D.K. Peeler, M.J. Plodinec, J. Nucl. Mat. 378 (2008) 244–256.
[47] B. Grambow, R. Muller, J. Nucl. Mat. 298 (2001) 112–124.
[48] Y. Minet, B. Bonin, S. Gin, P. Frugier, J. Nucl. Mat. 404 (2010) 178–202.
[49] T. Advocat, J.L. Crovisier, J.L. Dussossoy, E. Vernaz, Effects of MgO on the short- and long-term stability of R7T7 and M7 nuclear waste glass in aqueous media, in: C.G. Interrante, R.T. Pabalan (Eds.), Scientific Basis for Nuclear Waste Management XVI, Mat. Res. Soc., Pittsburg, PA, 1993, pp. 177–182.
[50] E. Curti, J.L. Crovisier, G. Morvan, A.M. Karpoff, Appl. Geochem. 21 (2006) 1152–1168.
[51] D. Arniaud, C. Dupuy, J. Dostal, Chem. Geol. 45 (1984) 263–277.
[52] J.C. Parneix, J.C. Petit, Chem. Geol. 89 (1991) 329–351.
[53] M.P. Turpault, G. Berger, A. Meunier, Eur. J. Mineral. 4 (1992) 1457–1475.
[54] J.L. Crovisier, E. Vernaz, J.L. Dussossoy, J. Caurel, Appl. Clay Sci. 7 (1992) 47–57.
[55] S. Fiore, F.J. Huertas, F. Huertas, J. Linares, Clay Mineral. 36 (2001) 489–500.
[56] O. Ménard, T. Advocat, J.P. Ambrosi, A. Michard, Appl. Geochem. 13 (1998) 105–126.

[57] M. Steinmann, P. Stille, W. Bernotat, B. Knipping, Chem. Geol. 153 (1999) 259–279.
[58] P. Jollivet, C. Den Auwer, J.M. Delaye, E. Simoni, J. Non-Cryst. Solids 353 (2007) 344–353.
[59] R.H. Byrne, J.H. Lee, L.S. Bingler, Geochim. Cosmochim. Acta 55 (1991) 2729–2735.
[60] J.H. Lee, R.H. Byrne, Geochim. Cosmochim. Acta 56 (1992) 1127–1137.
[61] P.C. Burns, R.C. Ewing, M.L. Miller, J. Nucl. Mat. 245 (1997) 1–9.
[62] E. Curti, R. Dähn, F. Farges, M. Vespa, Geochim. Cosmochim. Acta 73 (2009) 2283–2298.
[63] A. Barkatt, E.E. Saad, R. Adiga, W. Sousanpour, Al. Barkatt, M.A. Adel-Hadadi, J.A. O'Keefe, S. Alterescu, Appl. Geochem. 4 (1989) 593–603.
[64] J.C. Sang, A. Barkatt, Phys. Chem. Glasses 36 (1995) 95–100.
[65] J.C. Sang, A. Barkatt, J.A. O'Keefe, J. Non-Cryst. Solids 208 (1996) 170–180.